

Fault Diagnosis of Wind Turbine Gearboxes Using Enhanced Tachless Order Tracking

Mohamed A. A. Ismail¹, Nader Sawalhi² and Andreas Bierig¹

¹German Aerospace Centre (DLR), Institute of Flight Systems, 38108 Braunschweig, Germany

²SpectraQuest Inc., Richmond VA 23228, USA

Mohamed.Ismail@dlr.de, nsawalhi@spectraquest.com, Andreas.Bierig@dlr.de

Abstract— Health monitoring of wind turbines is crucial to support their sustainability and economic operation. Gearbox failures contribute significantly to the cost of wind turbine maintenance. These failures are typically monitored by vibration sensors attached to external housing. Non-stationary vibration is induced by the variable-speed operation of the wind turbine. In this paper, a new technique is introduced to enable the extraction of a speed reference from the vibration signal, which can be utilized to remove speed fluctuations and diagnose faults in the gearbox. High speed variations of the shaft, i.e., tacho signal, have been extracted from the vibration signal of an accelerometer mounted on the casing of the gearbox. The epicyclic mesh frequency has been used to construct the speed reference by an enhanced order tracking technique comprising auto-adjustable phase demodulation (APD). APD is aimed at improving fault detection efficiency by accommodating high speed fluctuations. The effectiveness of the proposed APD performance has been successfully demonstrated by using vibration measurements from commercial in-service wind turbines.

Index Terms— Computed order tracking, phase demodulation, planetary gearbox, non-stationary vibration

I. INTRODUCTION

Order tracking [1], which is commonly known as angular resampling, is a fundamental signal preprocessing algorithm to remove shaft speed fluctuations. This process requires a speed reference so that interpolation can be used to create a constant number of samples per shaft revolution (angular sampling) as opposed to temporal sampling. The speed reference is typically obtained using a tachometer or encoder sensors. In cases where a tachometer or encoder cannot be added, the vibration signal itself can be used to extract the speed reference [2]. Speed reference extraction, from the vibration signal itself, is normally obtained by using signal-phase demodulation, which is conducted on a frequency band around the fundamental shaft speed or one of its higher harmonics. Using a pseudo-tachometer as an alternative to the phase demodulation process was proposed in [3] with similar results. For this process to work there should be no overlapping from the higher harmonics. Thus, this process is best performed on the fundamental shaft frequency, in particular when the shaft has high-speed fluctuations, but it can then be repeated on higher harmonics to improve the result [4]. Once the order tracking process is done, the vibration frequency content (now in shaft orders) can be

processed further to diagnose different faults such as those in bearings or gears. Fig. 1 provides a block diagram describing this process.

In cases where high speed fluctuations, i.e. $>> 1\%$ [2], exist, as is typically seen in wind turbine signals, the signal processing becomes more challenging and is usually processed using short time intervals sections.

In this paper we propose an automated algorithm to extract a speed reference and speed profile for a wind turbine signal with high speed fluctuations (around $\pm 13\%$ of the mean speed). Due to the nature of the signal, the fundamental shaft frequencies and their harmonics were not suitable for phase demodulation.

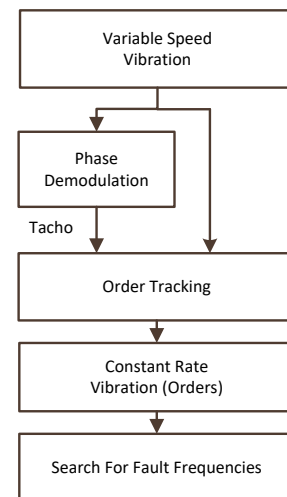


Fig. 1. Block diagram for tachless order tracking based fault detection

The gear mesh frequencies for the helical gear stages were smeared and thus were also not suitable for pseudo-tachometer extraction. Instead a frequency band around the epicyclic gear mesh frequency was selected and the tracking of the high-speed shaft was obtained by scaling the epicyclic gear mesh using the number of teeth. Envelope analysis was then used on the processed signal to diagnose the bearing fault.

This paper is organized in five sections. Section II gives an overview of the order-tracking stages, including principles and limitations of the phase demodulation band stage. Section III describes a new adjustable technique for phase demodulation. Section IV shows the experimental validation for proposed technique for in-service wind data. The overall contributions are summarized in Section V.

II. ORDER TRACKING

A. Principle

Order tracking is the process of transforming transient vibrations measured during variable-speed operation into ordered vibrations, estimated in the constant rate angular domain [1]. This paper uses the computed order tracking (COT) technique described in [5]. COT uses multiples of the running speed (i.e., orders), instead of absolute frequencies (i.e., Hz). This is useful for health monitoring, since COT can help isolate speed-related vibrations, such as those that occur due to faults in bearings and gears.

To use order-tracking analysis, the vibration signal must be sampled at constant increments of the relative rotor shaft angle $\theta(t)$, which is obtained from a tachometer. The next step of the order tracking is to interpolate the variable-speed vibration Acc_i , synchronized by $\theta(t)$, into the ordered vibration Acc_o , synchronized by $\theta_o(\theta)$, as given by (1):

$$Acc_o(\theta) = \text{Interpolation}(\{\theta(t), Acc_i\}, \theta_o(\theta)) \quad (1)$$

To extract the health characteristic frequencies, the signal envelope of the ordered vibrational acceleration Acc_o is determined using, for examples, the Hilbert transform.

B. Phase Demodulation Method

Phase demodulation (PM) is a technique for extracting instantaneous angular speed (IAS) by locating a specific synchronized frequency band (SFB) that comprises the harmonic of the shaft speed as shown in Fig. 2. Detailed investigations for PM principles can be found in [3].

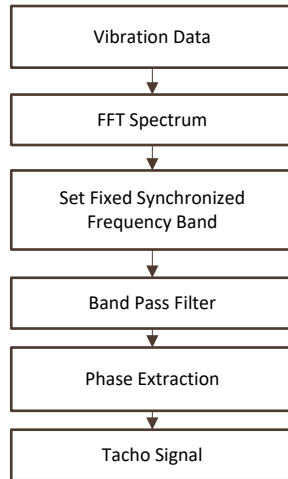


Fig. 2. Overview of phase demodulation method

This frequency band contains shaft-speed variability, encoded by the phase angle of SFB. In some conditions, such variability may exceed SFB limits and thus an incorrect tachometer signal may be obtained. However, increasing SFB width may lead to an incorrect tachometer signal by including transients that are non-synchronized with shaft speed. A new criterion for defining optimum SFB, based on adjustable phase demodulation (APD), is proposed in the next section.

III. ADJUSTABLE PHASE DEMODULATION

We investigate the tachometer signal extracted via the fixed PM method in Section IV.C. Fixed PM assumes that speed variability can be tracked by a fixed demodulation band. This principle is feasible if two conditions are satisfied: first, rotor speed variability is less than PM's width; second, maximum rotor speed variability is approximately centered at band half-width i.e. as a peak. We found that band pass filtration is sensitive to unbalanced frequency bands. As shown in Fig. 3, unbalanced bands, (B) could offset extracted speeds by comparing to balanced bands (A).

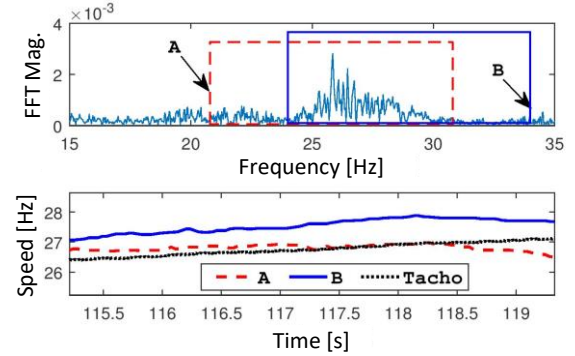


Fig. 3. Example of a phase demodulation using: (A) a balanced band around spectrum's peak and (B) an unbalanced band.

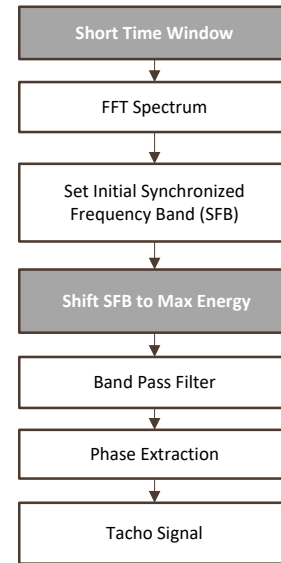


Fig. 4. Overview of APD stages

A proposed solution is introduced here by monitoring the demodulation bands prior to band pass filtration to keep them balanced. The initial frequency band is used for searching for the maximum peak. This step is necessary because the initial band was selected to track a specific characteristic frequency (e.g., gear mesh or rotor unbalance). The essence of the proposed algorithm is illustrated in Fig. 4.

IV. CASE STUDY: CMMNO CHALLENGE

A. Challenge Overview

Wind turbine vibration signals were provided by the organizers of the International Conference on Condition Monitoring of Machinery in Non-stationary Operation (CMMNO 2014) [6]. The contest was supported by *Maia Eolis*, who kindly provided wind turbine signal (2 MW with three-stage gearbox). The speed of the main shaft (supporting the blades) varied between 13 and 15 rpm during the recording. The vibration signals were measured with a defective bearing and high speed fluctuations. A schematic presentation of the two helical stages of the gearbox and the planetary stage is shown in Fig. 5. The kinematic information for the different shaft, gear, and bearing fault frequencies are provided in Tables I and II.

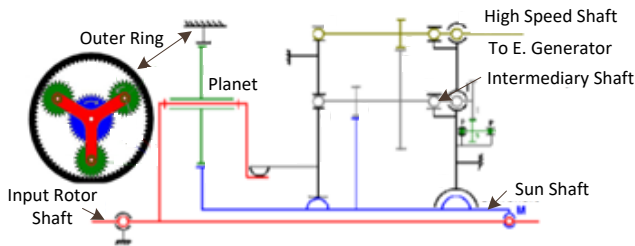


Fig. 5. Drivetrain of a commercial wind turbine involving a planetary gearbox and supporting ball bearings [6]

TABLE I
KINEMATIC SPEEDS BASED ON ROTOR INPUT OF 13–15 RPM

Item	Speed in Hz
Main Rotor Speed	0.22–0.25
Low-Speed Shaft (LSS)	1.49–1.72
Intermediate-Speed Shaft (ISS)	6.28–7.25
High-Speed Shaft (HSS)	25.99–30.00
Gear Mesh Frequency	
Epicyclic (GMF2)	26.65–30.75
1st stage (GMF1)	138.2–159.5
2nd stage	753.7–869.7

TABLE II
BEARING FAULT FREQUENCIES BY 13 RPM INPUT SPEED

	HSS [Hz]	ISS [Hz]	LSS [Hz]
BPFO	173.97	42.04	9.95
BPFI	241.85	58.45	13.83
FTF	10.40	2.51	0.59
BSF	77.47	18.72	4.43

The objectives of analyzing the wind turbine vibration data are:

- Extracting the instantaneous speed of the high-speed shaft using the vibration signal (carrying gear #7)
- Identifying the faulty bearing, where bearing fault characteristic frequencies are given in Table II.

B. Data Exploration

The raw vibration signal is depicted in Fig. 6, while Fig. 7

shows the short-time Fourier transform (STFT) spectrogram of the provided signal. The speed profile can be seen clearly. Examples of synchronized harmonics are indicated by two arrows in Fig. 7. The families of presented frequencies are briefly traced through Fig. 8. The epicyclic mesh frequency (GMF2) and its harmonics can be seen in the low frequency part in Fig. 8. The same figure also shows the presence of the first three harmonics of the first-stage gear mesh frequency (GMF1).

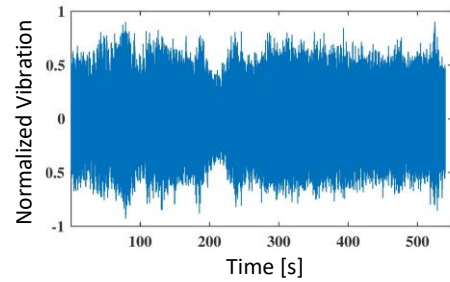


Fig. 6. Raw vibration signal from an accelerometer attached to planetary gearbox

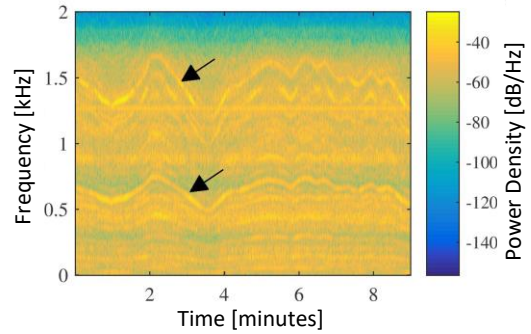


Fig. 7. Spectrogram for provided vibration signal

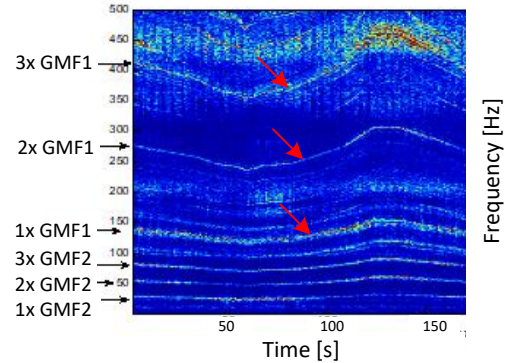


Fig. 8. Zoomed spectrogram of Fig. 7

C. Fault Diagnosis by Fixed-Phase Demodulation

The process to extract the speed profile of the high-speed shaft was carried out with the aid of the epicyclic mesh frequency (GMF2). This was appropriate as this is a dominant frequency, with no interference from other harmonics or sidebands, as shown in Fig. 9. The frequency band around the epicyclic gear mesh was isolated and inversely transformed to the time domain. The FFT of the signal zoomed in between 0 and 70 Hz is shown in Fig. 9. The demodulation band between 20 Hz and 30 Hz was selected. The noisy and smoothed (using a median filter) HSS profiles are shown in Fig. 10. The obtained profile closely matches the actual IAS profile.

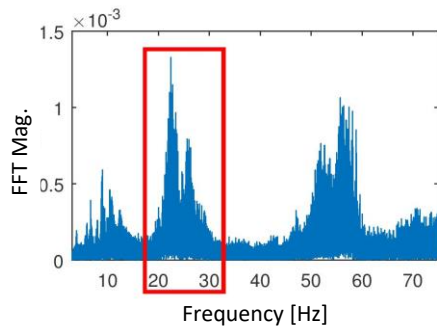


Fig. 9. FFT spectrum of full vibration data with a demodulation band of 20–30 Hz to include GMF2 range

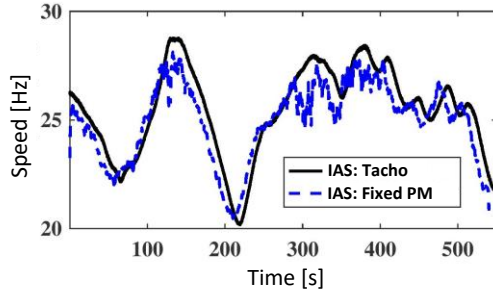


Fig. 10. Extracted IAS compared to actual IAS from a tacho-generator.

D. Fault Diagnosis by Adjustable Phase Demodulation

The vibration data is divided into 10% overlapped time windows of 20 seconds interval. It was selected based on Fig. 8, where harmonics have tolerable fluctuations within 20 seconds. An initial frequency band of 20 to 30 Hz is utilized for all windows, similar to Section C. For each window, the FFT spectrum is examined at the initial 20–30 Hz band. If the spectrum is not centered within the initial band, a new frequency band is selected around the maximum peak of the initial band, as shown in Fig. 11.

Fig. 12 shows the instantaneous adjusted demodulation band along vibration duration. A significant variation of the demodulation band can be observed. Variable demodulation bands are then filtered independently for each window to extract IAS through the corresponding phase angle.

The results of applying adjustable phase modulation are depicted in Fig. 13. The Adjustment of the demodulation band significantly enhances the IAS estimation, in particular for rapid speed fluctuations. This can be evaluated by calculating the IAS tracking error, which is the maximum instantaneous difference between the actual and extracted IAS signals. Adjustable modulation and fixed modulation achieve 4.5% and 12% error, respectively. The tracking error for fixed modulation is close to the provided speed fluctuation ratio of 13% for the wind turbine challenge.

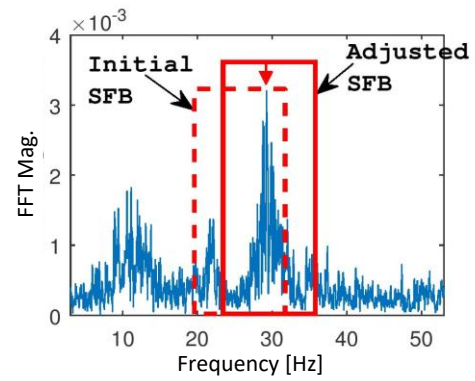


Fig. 11. Example of FFT spectrum of a short time window is shown. The initial SFB (20–30 Hz) no longer bounds the major harmonic peak and an adjusted SFB is used.

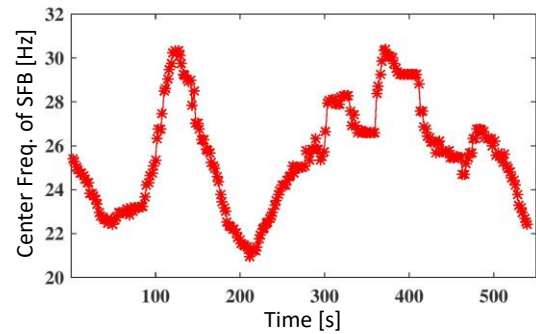


Fig. 12. Instantaneous adjusted SFB presented by its center frequency is shown for whole vibration signal.

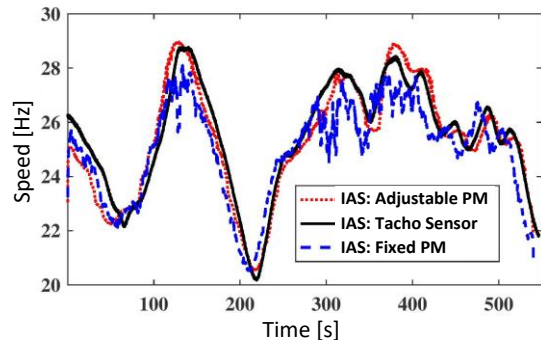


Fig. 13. IAS signals from: a tacho sensor, a fixed demodulation band (PM) and an adjustable PM are depicted to evaluate different speed-extraction methods.

Different sections of the signal with limited speed variation were analyzed and a squared envelope analysis was performed on these time sections. The advantages of using a squared envelope over other envelope types have recently been investigated in [7].

The one result (see the band selected in Fig. 14), which gave somewhat close correspondence to a fault characteristic frequency (FCF) at 0.73 is shown in Fig. 15. This FCF approximately matches $BPF1 \cdot (LSS/HSS) = 13.83 \text{ Hz} \cdot (1.49 \text{ Hz}/25.99 \text{ Hz}) = 0.79$, i.e. an inner race fault in the low-speed shaft, which is confirmed by its side bands. This agrees with the reported fault in the defective bearing of this wind turbine.

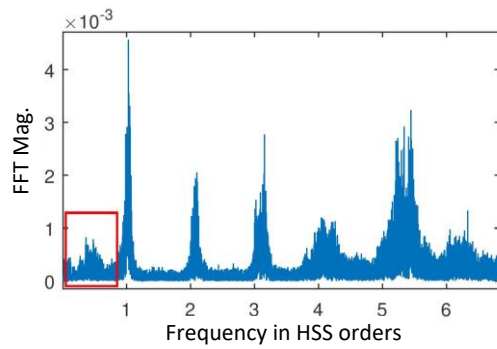


Fig. 14. Resampled FFT spectrum

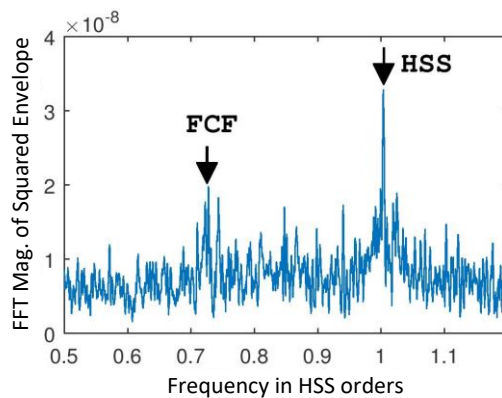


Fig. 15. Squared envelope FFT spectrum is shown after resampling the vibration signal. Fault characteristic frequency (FCF) at 0.73 order is detected with significant sidebands, that indicate BPFI at LSS.

V. CONCLUSION

Phase demodulation (PM) is a well-known technique for tracking rotor speed from non-stationary vibration. However, PM is limited by rapid speed fluctuations that are unavoidable for wind turbines due to irregular airflow. Adjustable phase demodulation (APD) has been introduced to overcome such deficiency by adding two stages to PM. The first is to divide vibration data into short overlapped time windows prior to obtaining the FFT spectrum. The second stage is to shift the demodulation band of each window to have better balanced energy, i.e., to make the highest peak centered in the frequency band. The performance of APD versus PM has been evaluated via an in-service wind turbine vibration with a defective bearing. The APD achieved 4.5% maximum tracking error compared to a tachometer signal, while PM gave a 12% error. In addition, APD enhanced fault diagnosis by providing more accurate speed measurements to identify an inner race bearing fault in the low-speed shaft.

REFERENCES

- [1] K. R. Fyfe and E. D. S. Munck, "Analysis of computed order tracking," *Mechan. Syst. Signal Proc.*, vol. 11, no. 2, pp. 187–205, Mar. 1997.
- [2] F. Bonnardot, M. El Badaoui, R. B. Randall, J. Danière, and F. Guillet, "Use of the acceleration signal of a gearbox in order to perform angular resampling (with limited speed fluctuation)," *Mechan. Syst. Signal Proc.*, vol. 19, pp. 766–785, 2005.
- [3] J. Urbanek, T. Barszcz, N. Sawalhi and R. Randall, "Comparison of amplitude-based and phase-based methods for speed

tracking in application to wind turbines," *Metrol. Meas. Syst.*, vol. 18, no. 2, pp. 295–304, 2011.

- [4] M.D. Coats and R.B. Randall, "Single and multi-stage phase demodulation based order-tracking," *Mechan. Syst. Signal Proc.*, vol. 44, no. 1, pp. 86–117, 2014.
- [5] K. Wang and P. S. A. Heyns, "A comparison between two conventional order tracking techniques in rotating machine diagnostics," *Int. Conf. Qual., Reliability, Risk, Mainten., Safety Eng. (ICQR2MSE)*, Xi'an, China, June 2011.
- [6] CMMNO'14 diagnosis contest, *Int. Conf. on Condition Monitoring of Machinery in Non-Stationary Operation*, Lyon, Dec. 2014, https://cmmno2014.sciencesconf.org/conference/cmmno2014/pages/cmmno2014_contest_V2.pdf.
- [7] M. S. Islam, F. S. Chowdhury, J. Lee and U. Chong, "Comparison of square and Hilbert based envelope Analysis based on background noise," *Int. Journal of Industrial Electronics and Electrical Eng.*, vol. 4, no. 10, pp. 57–61, Oct. 2016.